# Deep-Injection and Closely Monitored Induced Seismicity at Paradox Valley, Colorado

by Jon Ake, Kenneth Mahrer, Daniel O'Connell, and Lisa Block

**Abstract**   The U.S. Bureau of Reclamation's Paradox Valley Unit (PVU) extracts aquifer brine from nine shallow wells along the Dolores River, Paradox Valley, in southwestern Colorado and, after treating, high pressure injects the brine 4.3–4.8 km below the surface. PVU injects at rates between ~800 and ~1300 L/min. Since 1991, PVU has emplaced over $4 \times 10^6$ m$^3$ of fluid and induced more than 4000 surface-recorded seismic events. The events are recorded on the local 15-station Paradox Valley Seismic Network. The induced seismicity at Paradox separates into two distinct source zones: a principle zone (>95% of the events) asymmetrically surrounding the injection well to a maximum radial distance of ~3 km, and a secondary, ellipsoidal zone, ~2.5 km long and centered ~8 km northwest of the injection well. The expansion of these zones has stabilized since mid-1999, about three years after the onset of continuous injection. Within the principal zone, hypocenters align in distinct linear patterns, showing at-depth stratigraphy and the local Wray Mesa fracture and fault system. The primary faults of the Wray Mesa system are aseismic, striking subparallel to the inferred maximum principal stress direction, with one or more faults, probably, acting as fluid conduits to the secondary seismic zone. Individual seismic events, in both zones, do not discernibly correlate with short-term injection parameters; however, a 0.5 km$^2$ region immediately northwest of the injection well responds to long-term, large-scale changes in injection rate and the surpassing of a threshold injection pressure. Focal mechanisms of the induced events are consistent with simple double-couple, strike-slip moments and subhorizontal extension to the northeast. In addition, the fault planes are consistent with principal stress directions determined from borehole breakouts. More than 99.9% of the PVU seismicity is below human detection (~**M** 2.5). However, approximately 15 events have been felt locally, with the largest being a magnitude **M** 4.3. Because of the **M** 4.3 and two earlier-felt **M** ~3.5 events and injection economics, PVU changed injection strategies three times since 1996. These changes reduced seismicity from ~1100 events/year to as low as ~60 events/year.

## Introduction

Deep-well injection can induce seismicity (Nicholson and Wesson, 1990; Baisch *et al.*, 2002). Most injections are either low- to moderate-pressure (i.e., below fracture pressure), long-term injections (e.g., enhanced oil and gas recovery), which typically induce minimal seismicity that can be recorded on the surface; or high-pressure, short-term injections (e.g., hydraulic fracturing), which also rarely trigger seismicity that can be recorded at the surface. However, a few documented cases of continuous, high-pressure, long-term fluid injections have induced seismicity that was recorded at the surface (Nicholson and Wesson, 1990). Among these are the injections at Rocky Mountain Arsenal near Denver, Colorado (Healy *et al.*, 1968) and near Rangely,

Colorado (Raleigh *et al.*, 1972). At the Arsenal, Evans (1966) reported more than 1300 surface-recorded events induced by injection into crystalline basement rock 3.67 km below the surface at a maximum surface pressure of ~72 MPa. More than $6.2 \times 10^5$ m$^3$ of fluid were injected over 47 months. Healy *et al.* (1968) estimated deviatoric stresses at the bottom of the injection well to be ~47 MPa. Hseih and Bredehoeft (1981) and Zoback and Healy (1984) estimated a fluid pressure increase of 3.2 MPa was sufficient to induce the seismic activity. The largest event at the Arsenal, an **M** 5.3, occurred several kilometers from the injection well more than a year after injection ended. The motivation for the Arsenal injection was the disposal of unwanted fluids.

A similar type of injection is presently occurring in a remote location in Colorado.

Excess salinity in the Colorado River causes hundreds of millions of dollars in damage and difficult political issues for the seven states of the river's basin (Colorado, New Mexico, Utah, Arizona, Wyoming, Nevada, and California), and for Mexico. One significant natural point source of salt influx is the shallow, Paradox Valley aquifer in southwestern Colorado (Fig. 1). The ground water, Paradox Valley Brine (PVB), is saline-saturated (260,000 mg/L) and, if unabated, seeps into the Dolores River, a tributary of the Colorado River, at a rate of $\sim 2 \times 10^5$ ktonnes of salt per year. In the mid-1970s, the U.S. Bureau of Reclamation initiated the Paradox Valley Unit (PVU) to reduce the salinity of the Dolores River. Since 1991, PVU has high-pressure injected more than $4 \times 10^6$ m$^3$ of the aquifer brine, which has included more than $9 \times 10^5$ tonnes of salt, into deep Paleozoic and Pre-Cambrian strata. The injection has induced over 4000 surface-recorded, seismic events.

Finally, it is important to recognize that PVU is not a research operation, but an economically-governed project to remove and dispose of brine. Hence, the project has two goals: (1) maximize brine disposal while minimizing objectionable (i.e., felt) seismicity, and (2) characterize the res-ervoir (e.g., lifetime, injectability) within the parameters dictated by (1). Analyzing and interpreting the induced seismicity helps meet these goals.

Following is a case study of the first decade and a half of PVU operations. This includes a description of the facilities, including the Paradox Valley Seismic Network; the local geology; operations and seismic response; Mohr circle analysis; event locations and their illumination of local geological structures; a localized region seismically responsive to large-scale pressure changes; and earthquake recurrence, moment-injected volume, and focal mechanism analyses.

## Facilities

### The Paradox Valley Unit

PVU consists of nearly 100 shallow (10–100 m deep) wells, of which nine are brine extraction wells along the Dolores River near the center of Paradox Valley; surface filtration, treatment, transport, and pumping facilities; a U.S. Environmental Protection Agency (EPA)-permitted Class V, deep (total depth [TD] $\sim 4.9$ km) injection well—the world's deepest continuous disposal well; and a local seismic monitoring network, the Paradox Valley Seismic Network
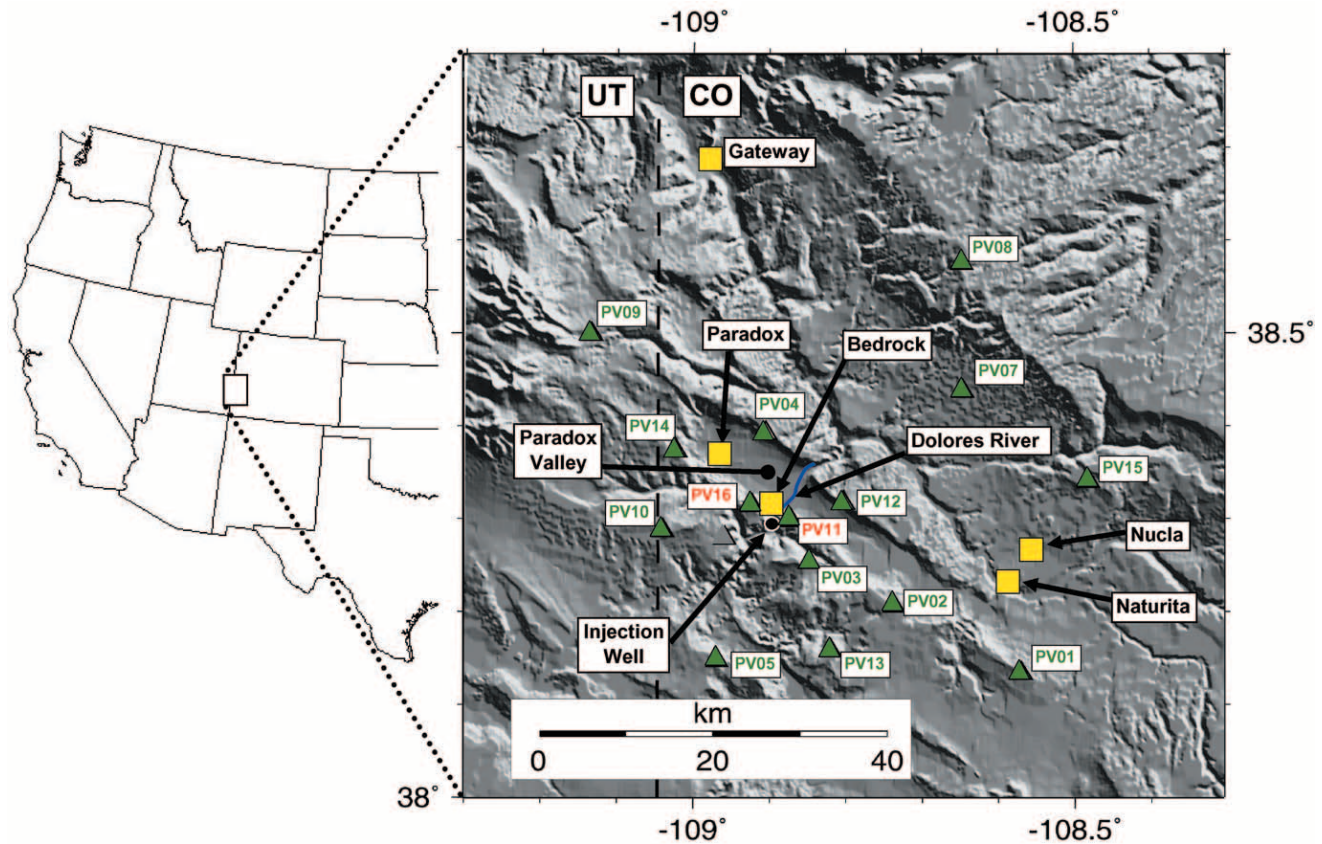


Figure 1. Paradox Valley Unit location map. Inset map shows Paradox Valley. Injection well (black circle), local municipalities (yellow squares), Dolores River across Paradox Valley (blue line), and Paradox Valley Seismic Network (green triangles; vertical-only stations, green lettering; 3-component stations red lettering).

(PVSN). The injection well is cased from the surface to TD with incoloy (a corrosion-resistant, nickel-based alloy) pipe, and perforated for injection between 4.3 km and 4.8 km below the wellhead. The wellhead is 1.52 km above mean sea level.

At the pumping facility, until January 2002, PVU diluted the PVB with fresh water to a 70% PVB–30% fresh water injectate ratio. Brine dilution resulted from concerns that 100% PVB injection would precipitate excessive calcium sulfate at depth and block injection (Karakha *et al.*, 1997). In late 2001, PVU reexamined this threat and considered it sufficiently reduced after years of injection to inject 100% PVB. In January 2002, PVU began injecting 100% PVB, which continues to present with no evidence of significant precipitation.

Throughout its history, PVU has used matched, constant-rate injection pumps; the individual injection rate of the present generation of pumps is ∼430 L/min. With this style of pump, injection pressure is a variable, being a function of both injection rate and injectivity of the target formations.

From 1991 through 1995, PVU ran a series of injection tests to qualify for an EPA injection permit. Having been granted the permit in 1996, PVU began and sustains continuous (i.e., "round-the-clock") injection. Based on wellhead safety restrictions, the maximum sustained surface pressure is ∼34.5 MPa. (Note: Ignoring minor variations in the specific gravity of the different injectates, this surface pressure limit corresponds to ∼82+ MPa pressure at the top of the casing perforations. As a point of reference, the injected-determined, *in situ* fracture pressure at this depth is ∼70 MPa [EnviroCorp, 1995].) During the first ∼3 years of continuous injection, PVU frequently approached the wellhead safety limit, forcing unscheduled injection shut downs (i.e., hours to days) until diffusion of the injectate into the rock matrix sufficiently reduced the surface pressure.

### The Paradox Valley Seismic Network

Recognizing that sustained, deep, high-pressure injection could induce local earthquakes, in 1985, PVU installed the PVSN and began monitoring the local, pre-injection seismicity. PVSN has operated continuously since 1985 and gives coverage to ∼5500 km$^2$ of the Colorado Plateau centered on the injection well (i.e., the intersection of the Dolores River and west side of Paradox Valley, Fig. 1). Presently, PVSN operates 15 stations, loosely arranged in two concentric rings around the injection well; the outer ring has a nominal radius of ∼30 km (Fig. 1). The two closest stations operate three-component sensors; the remaining stations have only vertical-component sensors. At present, all sensors are Teledyne Geotech Model S-13s, a nominal 1-Hz sensor with a nearly flat response to 100 Hz (Geotech Instruments, www.geoinstr.com; last accessed February 2005). Besides the sensor, each site is equipped with an amplifier (bandpass: 0.2 to 25 Hz; gain: 60 or 78 dB, site-specific), voltage-control oscillator (Teledyne Geotech model 4250),

low-power telemetry radio, solar panel, batteries, and broadcast tower with antenna. In addition to the fifteen, high-gain velocity stations, PVSN operates two strong-motion accelerometers (Springnether FBA-23s recorded by Kinemetrics K2s), one near the injection well and one near the extraction wells. (Presently, the strong motion data are not normally included in event analysis.) All sites are located on the ground surface and have extremely low levels of cultural noise; this allows detection to **M** −0.5 and reliable location of **M** 0.5 events and above.

Each site broadcasts an analog signal to a local central receiver in Nucla, Colorado (Fig. 1). There the signals are digitized (100 samples/sec) and continuously transmitted via a digital telephone link to the processing center in Denver, Colorado. Here, a modified form of the EARTHWORM software package detects events, classifies, locates, calculates size (coda magnitude), and archives them. Subsequently each event is manually evaluated by a seismologist before being used in additional analyses. With regard to magnitude, the local coda magnitude relationship was originally calibrated to events recorded by USGS and University of Utah Seismic Networks.

Figure 2 shows four examples of (velocity) seismograms induced by injection and recorded by the PVSN system. Figure 2a is an **M** 0.9 event recorded 29 January 1994 at 20:19 UTC; Figure 2b, 7 February 1994 at 07:25 UTC, is the same magnitude and located 3 m from event (a); Figure 2c, 11 February 1997 at 12:04 UTC, is also an **M** 0.9 and located 9 m from (a); and Figure 2d, 30 October 1999 at 09:34 UTC, is an **M** 0.2 located 90 m from (a). Each of these seismograms has been bandpass-filtered between 0.5 and 20 Hz with a 4-pole, zero-phase Bessel filter.

### Local Geology

The Paradox Basin is located within the eastern Colorado Plateau near the Colorado-Utah border (Fig. 1). Historically, the region has exhibited very low levels of naturally-occurring seismicity (Ake *et al.*, 1994; Wong *et al.*, 1996; Ake *et al.*, 2002). Based on limited regional data, Zoback and Zoback (1980) suggested the current stress regime of the Colorado Plateau to be west-northwest directed compression.

Paradox Valley, located in the eastern portion of the Paradox Basin, is a collapsed diapiric salt anticline that trends ∼N55°W. The valley is ∼38 km long, 5–7 km wide, and underlain by up to 6 km of interbedded salts and shales of the Pennsylvanian-age Paradox Formation. The Dolores River crosses the valley about midway along its length. Before and after crossing the valley, the Dolores flows through deeply incised canyons.

PVU's primary injection target is the Mississippian-age Leadville Limestone, a locally vuggy, highly-fractured, very-tight dolomitic limestone at a depth of ∼4.3 km below the surface. The effective porosity (i.e., fracture porosity) is believed to be less than 6% (Bremkamp and Harr, 1988);
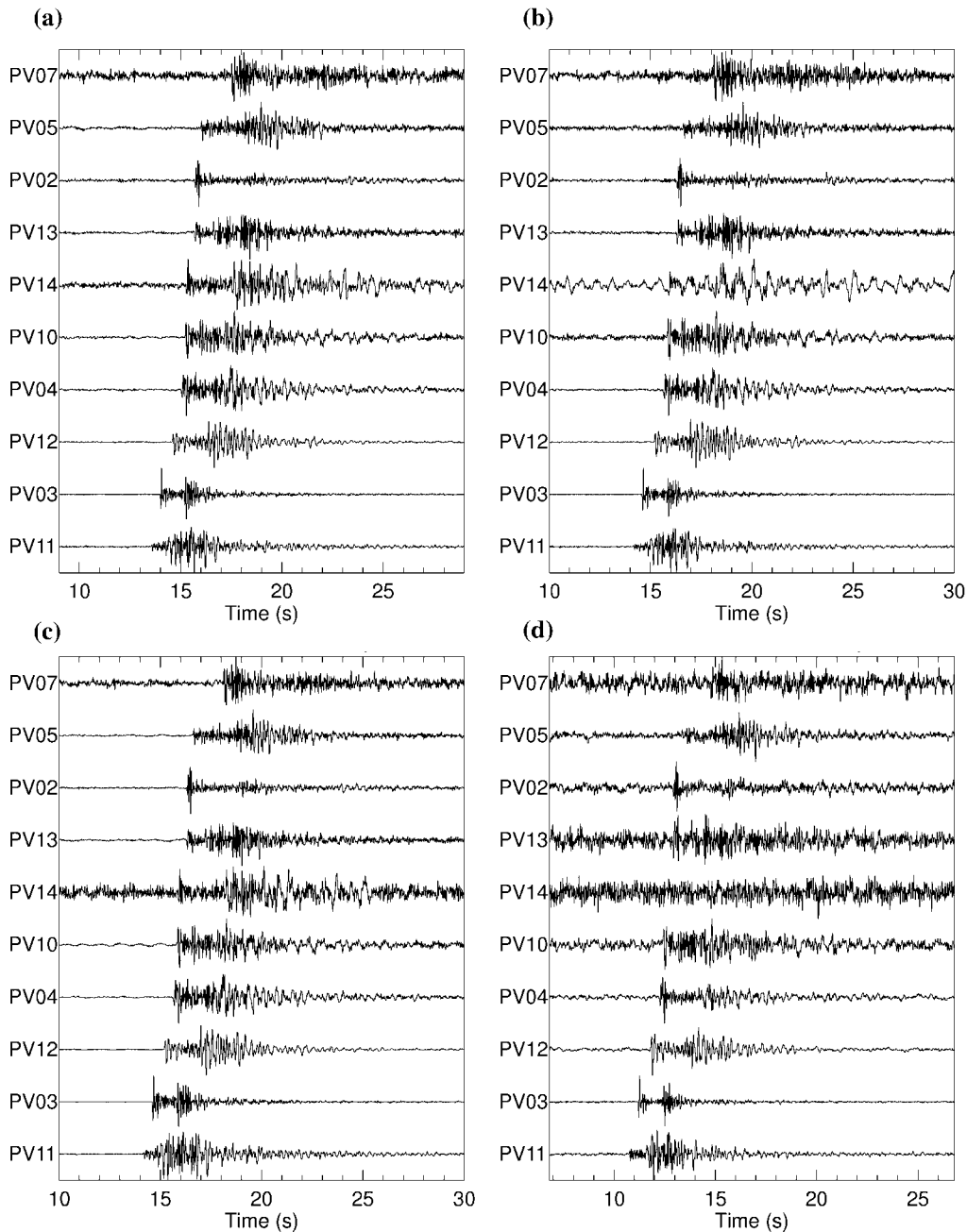
**Figure 2.** Examples of vertical-component seismograms from four closely-spaced seismic events recorded by the Paradox Valley Seismic Network. (a) An **M** 0.9 event recorded on 29 January 1994; (b) an **M** 0.9 located 3 m from (a) and recorded on 7 February 1994; (c) an **M** 0.9 located 9 m and recorded on 11 February 1997; (d) an **M** 0.2 located 90 m from (a) and recorded on 30 October 1999. These seismograms have been 0.5–20 Hz band passed filtered using a 4-pole, zero-phase Bessel filter.

however, widespread fracturing has significantly increased the local permeability. The injection interval (i.e., casing perforations) includes ~200 m of the Leadville Formation, underlying Devonian sandstones, and ~70 m of Precambrian aphanitic schist. Note that flow tests in the injection well (EnviroCorp, 1995) showed that most of the injection occurs at the upper portion of the perforation interval, which corresponds to the upper 20% of the Leadville Limestone formation.

Well logs from nearby wells, seismic reflection profiles, and site studies (Bremkamp and Harr, 1988) indicated a major series of Laramide-age step faults, the Wray Mesa fault system, trending subparallel to the strike of the Paradox Valley (~N55°W). These faults dip steeply to the northeast

while the strata shallow to the west-southwest. The injection well was sited to optimize fluid migration into and along these faults.

In addition to the Wray Mesa fault system, cores and fracture logs obtained during drilling, showed a well-developed fracture system in both the Leadville and Upper Precambrian. Harr (1988) found 55 m of recovered Leadville core contained 78 open fractures extending through ~15 m of core. He also states that well fracture logs indicated at least 58 m of probable Leadville fractures in contact with the wellbore, with fracture inclinations between 65° and 90°. Bremkamp and Harr's (1988) analysis of the recovered core and drill stem tests suggested brine transmission and storage would primarily depend on the lateral extent of the fracture field, since the primary porosity and permeability of the target horizons is low. Prior to construction of the injection well, Bremkamp and Harr (1988) analyzed existing deep wells in the Paradox Valley region and predicted a fluid gradient (i.e., fluid migration) to the northwest, within the Leadville Formation and along the postulated faults and fractures.

## Operations and Seismicity

At PVU, the injection operations divide into three main periods: Pre-Injection, Injection Tests, and Continuous Injection. As noted earlier, in response to objectionable seismicity and economic constraints, the Continuous Injection period subdivides into four phases; *Phase I* through *Phase IV*. These phases correspond to major and sustained changes in injection parameters.

### Pre-Injection, 1985–June 1991

In almost six years of monitoring prior to the first injection test in 1991, PVSN recorded and located only six natural earthquakes within ~19,000 km$^2$ surrounding the future injection site (Fig. 3). None of these events were within 10+ km of the injection well and none were large enough to be felt. This general lack of seismicity is consistent with previous observations in this part of the Colorado Plateau (Wong and Simon, 1981; Ake *et al.*, 1994).

### Injection Testing, July 1991–April 1995

Between July 1991 and March 1995, PVU conducted seven injection tests with durations ranging from 12 days to ~8 months (Table 1). The tests were required to qualify the well for an EPA Class V (i.e., non-hazardous liquid) disposal well permit. During these tests, PVU varied injection rate and injectate chemistry while measuring injection (surface) pressure and injection rate. Each injection test was followed by a shut-in period: the wellhead was closed and the pressure decline was recorded (EnviroCorp, 1995) for multiple days or longer. During the first week of the initial injection test, PVSN detected more than a dozen earthquakes within <1 km

of the well. Cumulatively, during and immediately after the seven injection tests, PVSN detected and located 666 induced events. Typically, seismicity ceased within hours to a few days following each test. The rapidity with which the earthquakes stopped seemed to correlate with the test duration. The characteristics of the injection tests (injection rate, initial pumping date and duration, injectate chemistry, and number of induced earthquakes) are summarized in Table 1. For this same time period, Figure 4 shows the injection rate and induced seismic events per day.

### Continuous Injection, May 1996–Present

Following the granting of the injection permit, PVU began continuous injection in May 1996, 13 months after the end of the injection tests. After about 100 days of injection adjustments and slowly increasing injection, the injection rate was fixed at ~1290 L/min at a (maximum) surface pressure of ~33 MPa. PVSN recorded its first induced seismic event associated with continuous pumping 111 days after pumping began. Between May 1996 and the end of 2003, PVSN recorded and located more than 3350 events within ~10 km of the injection well. Of these events, ~15 were reported felt at the surface (**M** ~2.5 or greater), with the first felt-event occurring in August 1997, more than a year after continuous pumping began. The injection rate, downhole pressure (i.e., pressure at 4.3 km depth), and seismic events per day versus time for this period are shown in parts (a) and (b) of Figure 5. In each of these figures, only events of **M** 0.0 and greater are included. In late 2000, a change in event-detection algorithm resulted in a reduced sensitivity for events less than **M** 0.0. For consistency, we include only the events at **M** 0.0 or greater for the entire data set. Of the more than 3350 events recorded since 1996, ~185 were less than **M** 0.0.

Figure 5 shows a number of characteristics, including profound changes in injection parameters (discussed later). Besides these changes, the figure shows that, despite the consistency in injection rate since mid 2000, the downhole pressure has consistently increased but, until the last half of 2003, the seismicity remained relatively low. The figure further shows that the downhole pressure since mid 2003 is the highest it has been since continuous injection began, but the noted increase in seismicity during the second half of 2003 is well below the 1998 and 1999 levels. The reason for this behavior is not apparent at this time.

In early June 1999, a magnitude **M** 3.6 event occurred that was strongly felt in the northwestern portion of Paradox Valley. Up to this point, the largest events were several **M** 2.8s, which were weakly felt in the immediately vicinity of the well. A month later, a second anomalously large event, a magnitude **M** 3.5, occurred. On 27 May 2000, the largest induced event at PVU, an **M** 4.3 event, occurred. This event was felt throughout the valley. Reports following this event noted minor rockfalls at cliff faces and, for several hours, altered flows in nearby springs. The strong motion acceler-
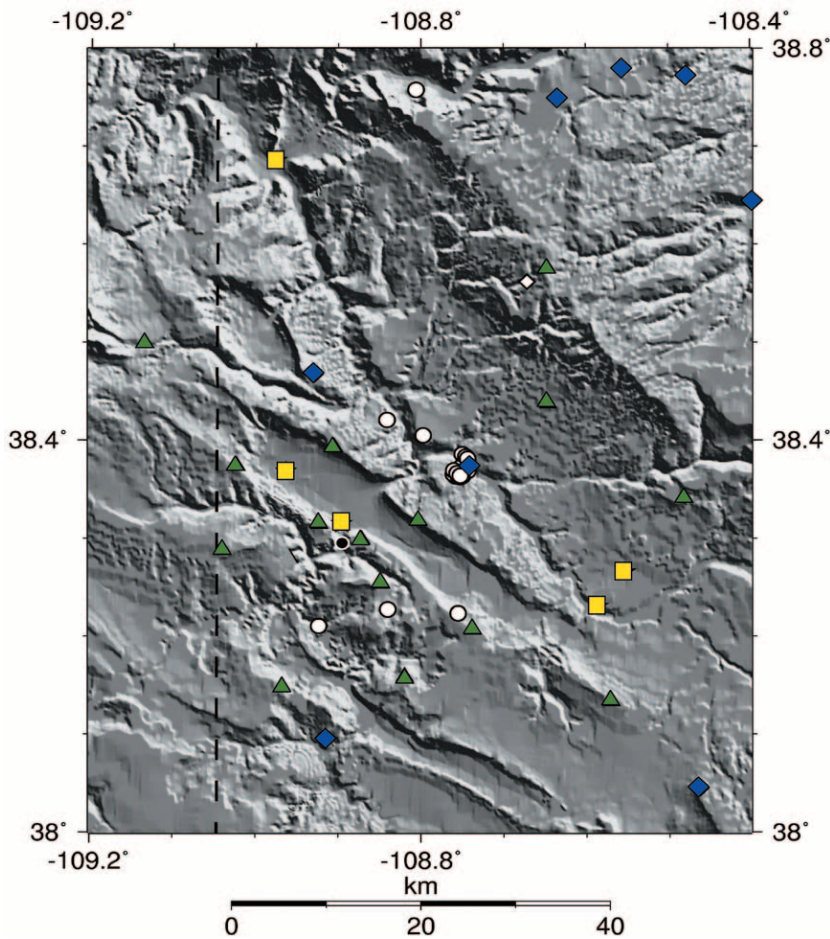
Figure 3. Paradox regional pre-injection seismicity, 1985–1991. Green triangles, Paradox Valley Seismic Network seismometer sites; yellow squares, local municipalities (see Fig. 1); black circle, injection wellhead; white circles, explosions; blue diamonds, natural seismic events.

Table 1
Injection Tests 1991–1995

| Test No. | Injected Volume m$^3$ | Initial Pumping Date and Duration (mm/dd/yy) Days | Injectate %PVB[b]:%Fresh Water | Hydrostatic Pressure at 4300 m[a] Depth (MPa) | No. Induced Seismic Events |
|---|---|---|---|---|---|
| 1 | 11,000 | (7/11/91) 14 | 0%:100% | 42 | 20 |
| 2 | 16,000 | (8/15/91) 12 | 33%:67% | 44 | 9 |
| 3 | 54,000 | (11/5/91) 54 | 67%:33% | 47 | 16 |
| 4 | 42,000 | (7/6/93) 47 | 0%:100% | 42 | 0 |
| — | 38 | | 28% HCl acid | | |
| — | 34 | (9/20/93) 14 | 100% fresh water flush following acid injection[c] | — | — |
| 5 | 54,000 | (10/3/93) 28 | 70%:30% | 47.2 | 81 |
| 6 | 89,000 | (1/18/94) 41 | 70%:30% | 47.2 | 170 |
| 7 | 354,000 | (8/14/94) 242 | 70%:30% | 47.2 | 370 |
| Total | 620,000 | 438 days | — | — | 666 |

[a]Depth = Top of the casing perforation interval (i.e., the top of the injection target horizon, the Leadville Limestone).

[b]PVB = Paradox Valley Brine (260,000 mg/L total dissolved solids).

[c]Injection well surface pressure became negative (i.e., below hydrostatic) following water flush of acid injection.
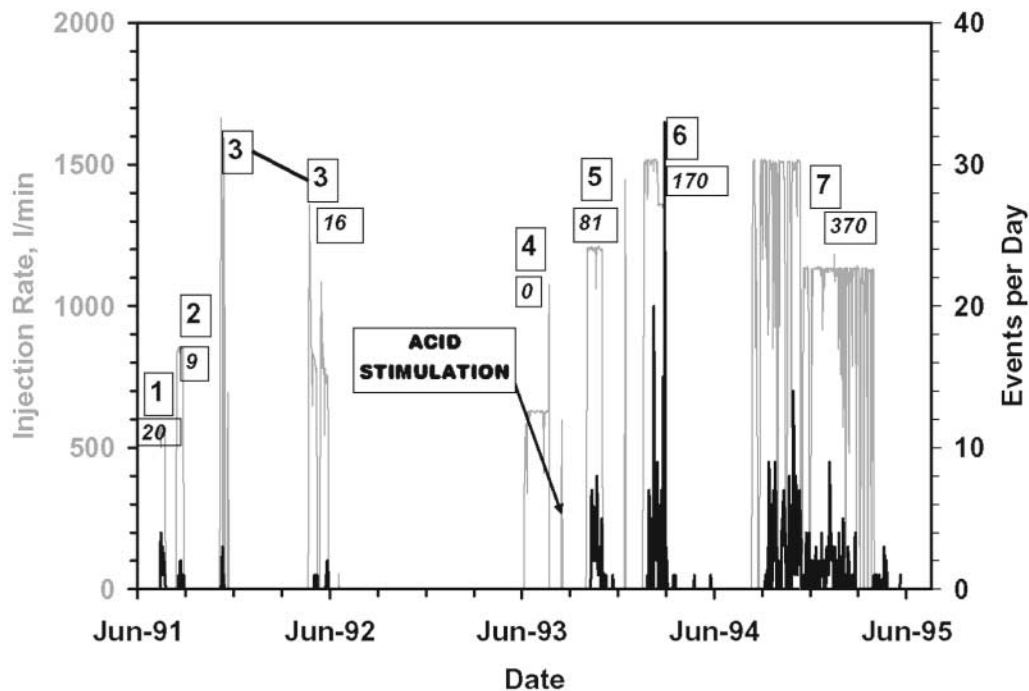
**Figure 4.**     1991–1995 injection test injection rate (gray, left axis) and induced earthquakes per day (black, right axis) versus time. Large boxed numbers indicate injection test number; smaller boxed numbers (italics) beneath large boxed numbers indicate number of seismic events induced by the corresponding test and recorded by PVSN.

ograph at the injection well recorded a peak horizontal acceleration of ∼0.3 g.

Because of these events and the need to maximize brine injection, PVU has instituted three operational changes since 1996. These changes result in four distinct operational phases (*Phase I* through *Phase IV*), as detailed in Table 2, Figure 6, and described in the following sections.

*Phase I (22 July 1996–25 July 1999, 1100 days).*     From July 1996 until after the two **M** 3+ events noted earlier, PVU injected 70% PVB:30% fresh water (specific gravity = 1.12) at its maximum capability: 1290 L/min and ∼33 MPa surface pressure. During this period, PVSN recorded its most robust seismicity (Table 2, Fig. 6). During *Phase I*, injection operations were punctuated by about 10, nominally short (1–10 days) unscheduled maintenance shutdowns and one major, 70-day facilities-upgrade shutdown (June and July of 1997). *Phase I* injection parameters (Table 2) were optimized for injection volume and wellhead safety. During this phase, we did not have sufficient data to put bounds on the recurrence of large seismic events. Prior to the **M** 3+s, as noted, the largest events were **M** 2.8s, barely large enough to be felt locally. The two **M** 3+ events forced PVU to reconsider and change injection strategy.

*Phase II (26 July 1999–23 June 2000, 332 days).*     Beginning in late July 1999, PVU instituted a strategy that included a 20-day shutdown every six months (in May and Decem-

ber–January). At the time we believed the shutdowns would control the proclivity to produce large events. We had observed that multi-day shut downs (i.e., hiatuses between the injection tests and during *Phase 1*) resulted in rapid decreases of seismicity and, following the resumption of pumping, a slow return in seismic rate. We hypothesized that the 20-day shutdowns would let the injectate diffuse from the potentially-active larger faults and fractures into the formation rock porosity (i.e., small fractures and pores). This would result in an increase in the locking stress (i.e., normal stress) across the larger faults and fractures. The scheduled shutdowns significantly reduced seismic event production (Table 2 and Fig. 6), however, shutdowns alone were not sufficient to reduce large event production to an acceptable level. As noted, on 27 May 2000, PVU witnessed its largest event, a magnitude **M** 4.3 event.

*Phase III (24 June 2000–7 January 2002, 566 days).*     The 27 May 2000, **M** 4.3 earthquake caused PVU to cease injecting for 28 days. When resumed, PVU began pumping at ∼870 L/min, a 33% reduced rate. This change further reduced overall earthquake production (Table 2 and Fig. 6) as well as larger event production. During *Phase I*, PVSN recorded an average of ∼81 earthquakes/month, with a peak of 172 events in January 1999. With the inception of *Phase III*, the seismicity rate decreased to ∼9 earthquakes/month, with no events over **M** 2.8. However, reducing injection volume 33% corresponds to reducing salt disposal 33%; salt
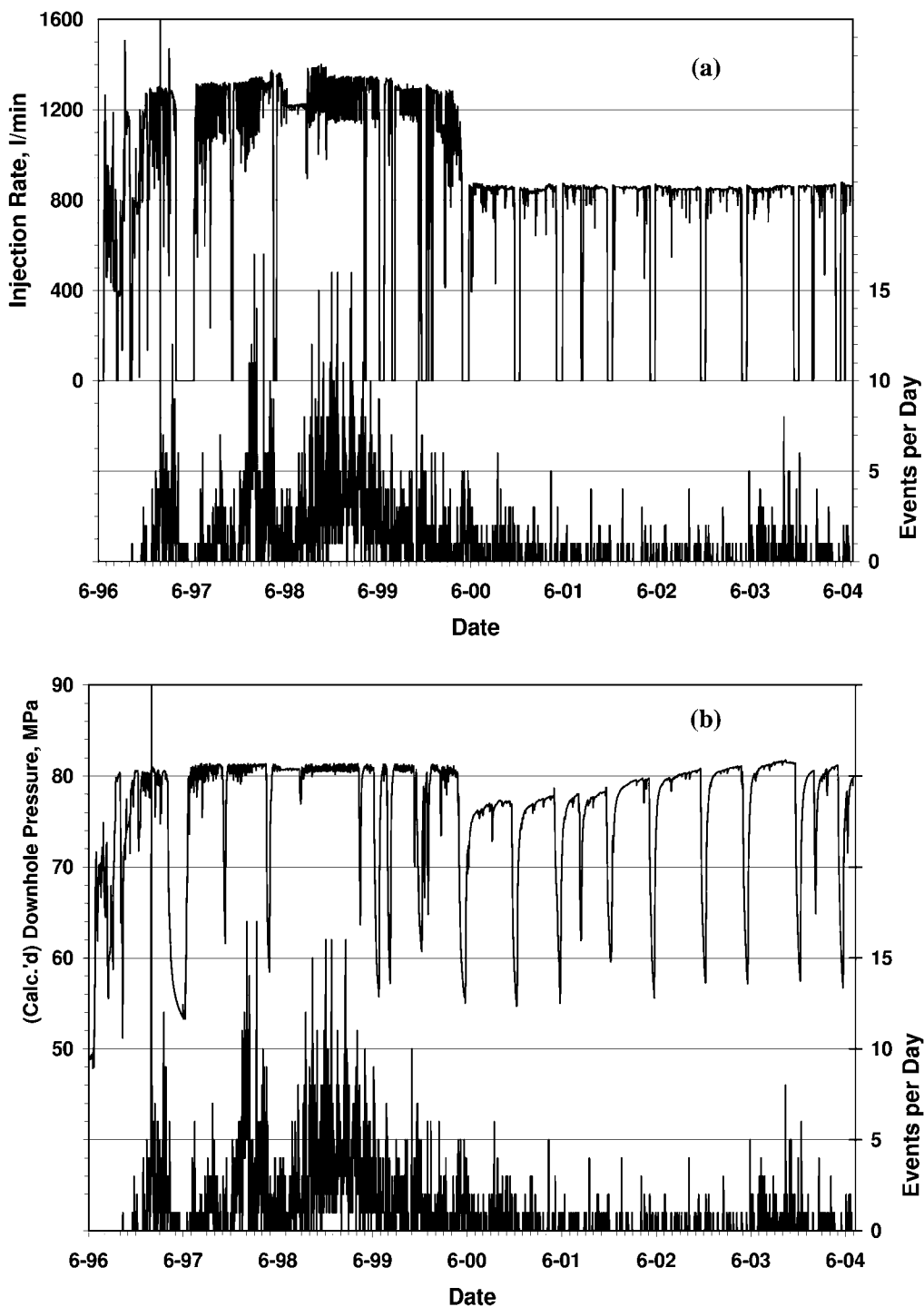
Figure 5.    (a), Daily average injection rate, and (b), daily average (calculated) down-hole injection pressure at 4.3 km depth below wellhead. Each graph shows events per day for continuous injection period 1996–2003.

disposal economics is the driver of the project. Hence, PVU considered alternatives and initiated *Phase IV* injection.

*Phase IV (8 January 2002–present, 724 days at the end of 2003).*    The results of a temperature log survey conducted in June 2001 suggested significant near-wellbore cooling had occurred over the previous six years of continuous injection. Since calcium sulfate precipitation is believed to be reduced significantly at temperatures below the observed pre-injection formation temperatures (Karakha *et al.*, 1997), in January 2002, PVU change injectate chemistry from 70:30 PVB-to-fresh-water to 100% PVB. This changed the specific

Table 2
Phases of Continuous Pumping

| Phases | Approx. Duration Days | Avg. Wellhead Pressure (MPa) | Avg. Pressure at 4.3 km[a] depth (MPa) | Avg. Inj. Rate[d] (L/min) | Injectate: %PVB: % H$_2$O | Biannual 20-Day Shutdown (Yes/No) | Approx. No. Seismic Events |
|---|---|---|---|---|---|---|---|
| I | 1100 | 33.8 | 80.7 | 1290 | 70:30 | No | 2446 |
| II | 332 | 33.8 | 80.7 | 1290 | 70:30 | Yes | 496 |
| III | 566 | 30.3 | 77.2 | 855 | 70:30 | Yes | 140 |
| IV | 724 +[b] | 30.3 +[c] | 79.3 +[c] | 855 | 100:0 | Yes | 277 |

[a]Depth = Top of the casing perforation interval, i.e., the top of the injection target horizon, the Leadville Limestone.

[b]Number includes days through 31 December 2003.

[c]Average pressure has been increasing following each 20-day shut-in.

[d]Average when pumping, does not include scheduled and unscheduled shut-downs.
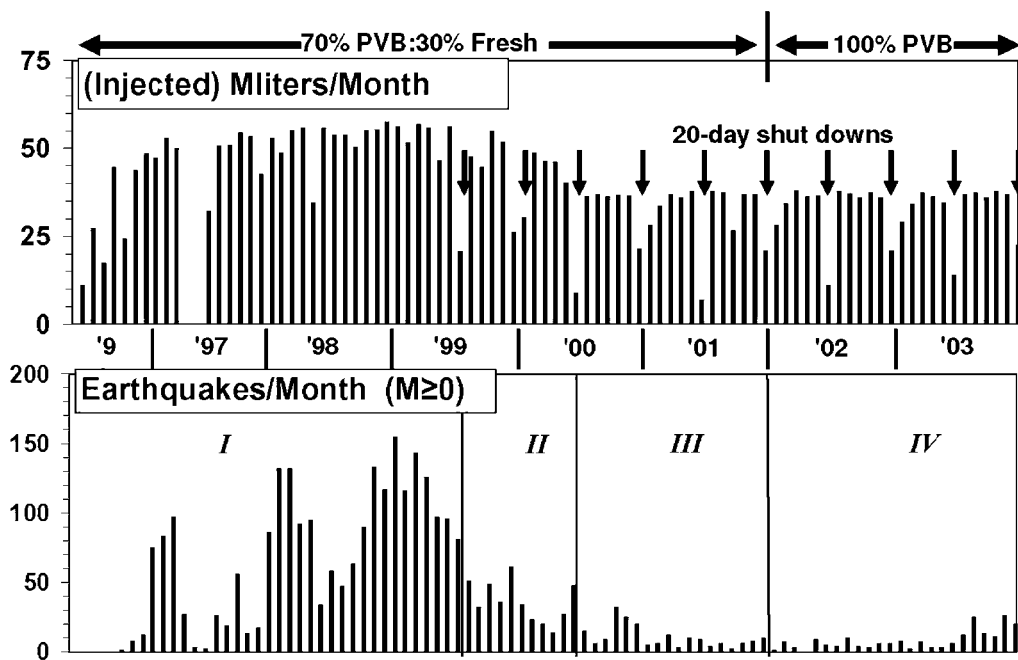


Figure 6.   Four phases of continuous pumping (1996–2003) superimposed on monthly injected volumes and induced seismic events per month versus time. PVB designates Paradox Valley Brine, the extract fluid from the local aquifer.

gravity of the injectate from 1.12 to 1.17 and correspondingly increased downhole pressure ~2 MPa at ~4.3 km (Table 2). A 100% PVB injection represents a 43% increase in disposed salt per unit volume over *Phases I–III*. To date we have noted no effects indicating significant precipitation.

## Mohr Circle and Initiating Seismicity

Following Cosgrove (1995), Figure 7 shows three Mohr circle estimates for the Paradox site at a depth of 4.3 km. We chose the 4.3-km depth because it is the upper portion of the Leadville limestone and the depth at which well testing indicated the majority of injection flow (EnviroCorp, 1995). Also shown in Figure 7 are the solid Navier-Coulomb criterion, which attaches to the (curved) Griffith criterion, and has a friction angle of 40°, shear (i.e., cohesion) strength of 21 MPa, and the dashed no-cohesion Navier-Coulomb failure criteria, which assumes the same friction angle. The values of the Navier-Coulomb criteria are for average, competent limestone (Hendron, 1968; Goodman, 1980). In Figure 7, the tensile strength for the Griffith criterion is assumed to be half the shear strength.

In Figure 7, circle number 1 is the state of stress inferred from the well logs and the inferred hydraulic fracture pressure (EnviroCorp, 1995) with no fluid pressure. The well logs yield a lithostatic (vertical) stress of ~103 MPa. Mini-hydraulic fractures performed after casing perforation yielded a (horizontal) least principal stress of ~69.6 MPa
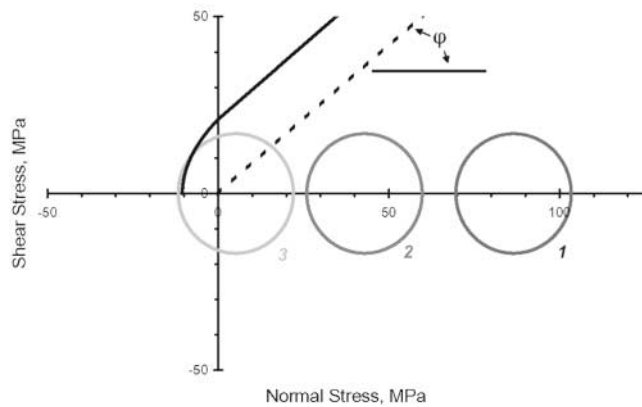
**Figure 7.** Mohr circle of Paradox Valley injection. Navier-Coulomb zero shear strength (dashed line) and Navier-Coulomb with shear strength (cohesion) and Griffith tensile (solid line) failure criteria indicated. A 40° friction angle for Leadville Limestone is assumed. Circle 1 includes stresses without fluids; circle 2 includes stress plus native aquifer pressure at ~4.3 km depth; circle 3 includes stress plus (downhole) injection pressure at the end of 2003 (81.4 MPa).

(J. Bundy, personal comm., 2004). The difference—the deviatoric stress—is ~33.4 MPa, a lower bound for the deviatoric stress. Circle 2 is circle 1 shifted toward the origin by the Terzaghi effective stress law (Goodman, 1980). The fluid pressure used for circle 2 is the Leadville Limestone (native) aquifer pressure at 4.3 km, ~43.6 MPa, (J. Bundy, personal comm., 2004). Circle 2 shows that the addition of the native aquifer fluid pressure is not sufficient to cause failure. This finding agrees with the lack of observed seismicity in this region. From Circle 2, an additional ~17 MPa (fluid) pressure is needed to shift the Mohr circle to tangency with the zero-strength Navier-Coulomb failure line. Hence, a downhole fluid pressure of ~60 MPa would be sufficient to induce shear failures across preexisting faults with orientations in or near the maximum shear plane.

In support of the ~60 MPa threshold as a lower bound on the initiation of slip, we examined the data from PVU's first two injection tests. We used these data since during these tests, the formation was in its native stress state, unaltered by subsequent large volume injections. During the third day of injecting, the downhole pressure reached ~64 MPa; on the fifth day of pumping, PVSN recorded it first induced event. During the thirteenth day, injection was stopped and the well shut-in; the downhole pressure was ~68 MPa; on the fourteenth day it had dropped to ~61 MPa; and the fifteenth it was down to 55 MPa. The last induced event recorded by PVSN for test 1 was on the thirteenth day of injecting. These results follow the ~60 MPa threshold noted earlier fairly well. Injection test 1 injected about 11,000 m³, a small enough volume to consider testing the ~60-MPa threshold on test 2.

Injection test 2 began about 3 weeks after test 1. Within two days of pumping, the downhole pressure was ~65 MPa,

and from there injection was held at or slightly above 70 MPa for the next 11 days. On the 12th day pressure dropped to ~65 MPa, then ~60 MPa the next day, and ~56 MPa on the next. PVSN recorded the first induced event in test 2 on the 4th day of the test. The last seismic event of test 2 occurred on the day when the downhole pressure went from 70 MPa to 65 MPa. The seismic results from tests 1 and 2 don't agree exactly, but they do agree to the extent than an approximately 60-MPa threshold is certainly a lower bound for the initiation of seismicity in the native Leadville limestone at the PVU site.

In support of our hypothesis—that with enough injection volume, the state of stress at PVU is altered—PVU downhole pressure went above ~60 MPa within about 30 days of the inception of continuous pumping in 1996. However, PVSN recorded the first induced event ~111 days after the onset of injection. At this time, the downhole pressure had reached ~80 MPa. This delay in the onset of surface-recorded seismicity may indicate that smaller events were induced, but their magnitudes were below the detection threshold of PVSN; or it may indicate that the volume injected during the seven tests (6.2 × 10⁵ m³) was sufficient to alter the in situ stress on favorably-oriented slip planes; or that the stress on these slip planes had already been reduced by the occurrence of previous events. For reference, circle 3 in Figure 7 uses the same principal stresses as circle 1 but includes a shift caused by the average downhole pressure at the end of 2003, 81.4 MPa.

As a final note on the Mohr circle analysis, the focal mechanism results discussed later show that the maximum principal stress is horizontal. Therefore the estimate of maximum principal stress based on the lithostat, described in this section, is a lower bound.

## Event Locations

To enhance our understanding of the induced seismicity, injectate and connate fluid flows, and pressure migration, we developed a highly-accurate method to locate the seismic sources. We began with a one-dimensional velocity model with station corrections. Subsequently we performed a three-dimensional velocity-hypocenter inversion that is followed by a relative relocation procedure. The details of the location procedures and enhanced accuracy are not given here, but are explained in a companion paper (Block *et al.*, unpublished manuscript).

The relocated events illustrate geological structures in the injection zone. These include stratigraphy (e.g., layering and dip), the major faults of the Wray Mesa system, and a non-symmetric network of minor faults and fractures communicating with the major faults. The relocated events strongly suggest fluid migration along this network of pathways away from the injection well (Fig. 8). These illuminated faults and fractures are not consistent with the traditional hydraulic fracture model of two flow paths: two vertical, symmetric fractures emanating from opposite sides
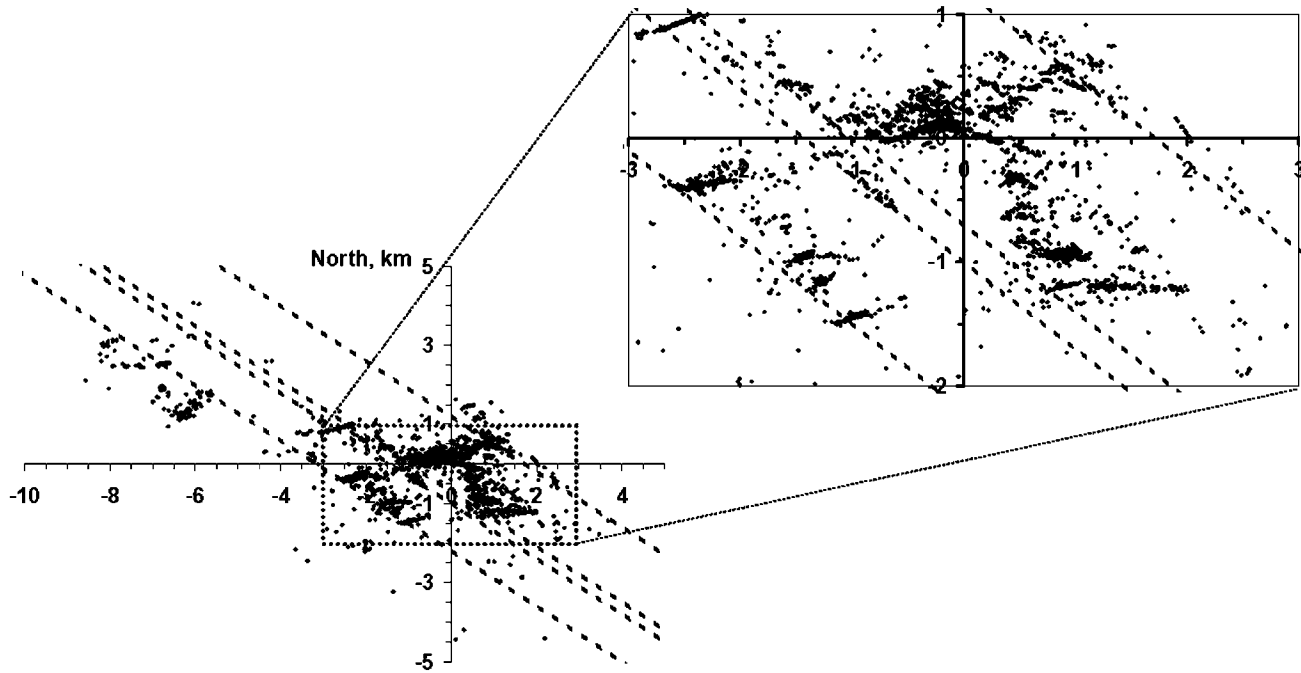
Figure 8.    Epicenter map of (relocated) induced seismicity includes close-up of near-wellbore events. Dashed lines show implied locations and strikes of primary faults of Wray Mesa fault system at the depth of Leadville Limestone.

of the injection well (e.g., Economides and Nolte, 1987; Mahrer, 1999). In addition to the illuminated fracture and fault network, Figure 9 shows the event locations are vertically confined to a relatively narrow depth range (3.5–6 km below surface), with the lateral extent of most events following the inferred depth interval of the target injection horizon; the Mississippian-age, Leadville Limestone (dips = ~10° to the east-northeast). (Note: Figure 9 shows a small number of very shallow events; we believe these to be mislocations.) Also, as noted in Figure 9, the deepest events occur unambiguously below the Leadville within the crystalline Precambrian rocks.

The inferred, asymmetric envelope surrounding the injection well and containing the induced seismicity grew noticeably throughout the injection testing period and continued through 1998, but has stabilized since 1998 (Fig. 10). Based on the microearthquake locations, we infer that fluid-pressure perturbations have migrated at least 8+ km from the injection well to the northwest. Consistent with the predictions of Bremkamp and Harr (1988), the direction of the furthest extending fluid migration seems to be to the northwest (Fig. 8), Bremkamp and Harr's direction of decreasing formation fluid pressure. As of the end of 2003, we have not been able to detect any correlation between (short-term) injection pressure behavior and the occurrence of individual events. However, we have noted a correlation between surface pressure history and a 0.5 × 0.5 km swarm of events adjacent to and northwest of the injection well (Fig. 11).

## Pressure-Responsive Seismic Swarm

As noted, we have not detected any direct correlation between individual earthquakes and formation pressure changes as seen through anomalous pressure changes in the surface (wellhead) pressure. However, a few times each year short-lived swarms occur. Typically these swarms are spatially compact (i.e., hypocenters within hundreds of meters or less) and lasting hours to a few days. With one exception, once they ceased, these swarms don't reactivate and, like individual events, they don't show any correlation with formation pressure changes. Recently we identified one swarm region of repeated, high-seismic activity and high responsivity to PVU's injection schedule changes. This 0.5 × 0.5 km swarm region is shown in Figure 11a as the boxed area. The zone covers an epicentral area of less than 3% of the cumulative, near-well epicentral envelope. Since 1996, 680 events, or ~18%, of the near-wellbore events have occurred in this zone. Figure 11b shows the seismic response of this region to downhole pressure. In the figure, the horizontal series of diamonds represent the occurrence times of events in the swarm zone. Two characteristics are obvious when comparing event occurrences and downhole pressure. First, when injection has been shut off (i.e., the sharp "drop outs" in the pressure in Fig. 11b), the swarm region very quickly shuts off. And, second, with very few exceptions, when the downhole pressure is below a threshold of ~80 MPa, the zone is quiet; when the pressure is above ~80 MPa, the zone
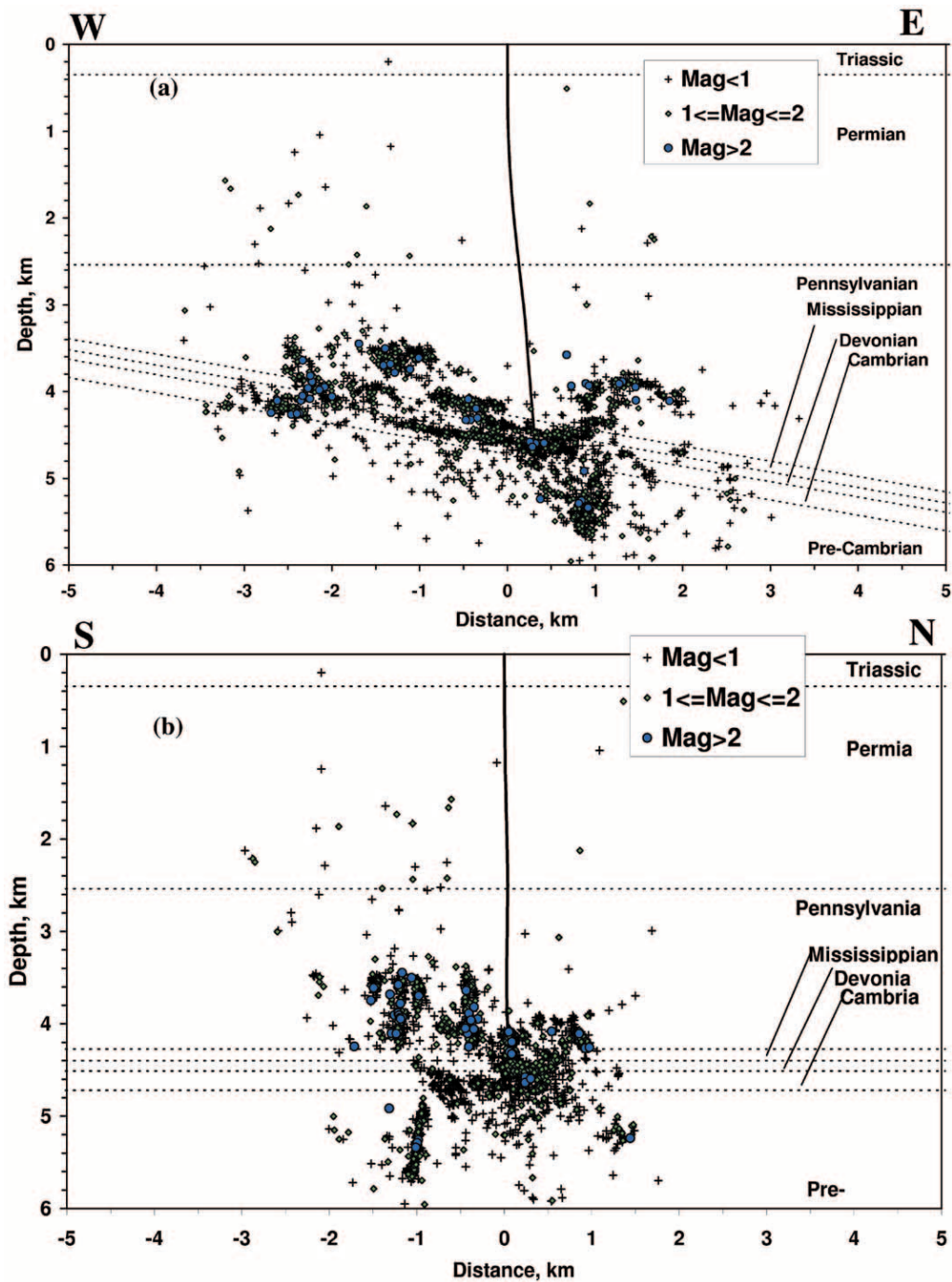
Figure 9. (a) East–West cross section of (relocated) induced seismicity viewed from the south looking north. (b), North–South cross section of (relocated) induced seismicity viewed from east looking west. The near-vertical line in center is the injection well. Also shown are the major stratigraphic units (Leadville Limestone is Mississippian) based on injection well logs. The dips are simple extrapolations from the wellbore and do not include stratigraphic offsets of the Wray Mesa faults. Depth is in kilometers, positive down from the wellhead.
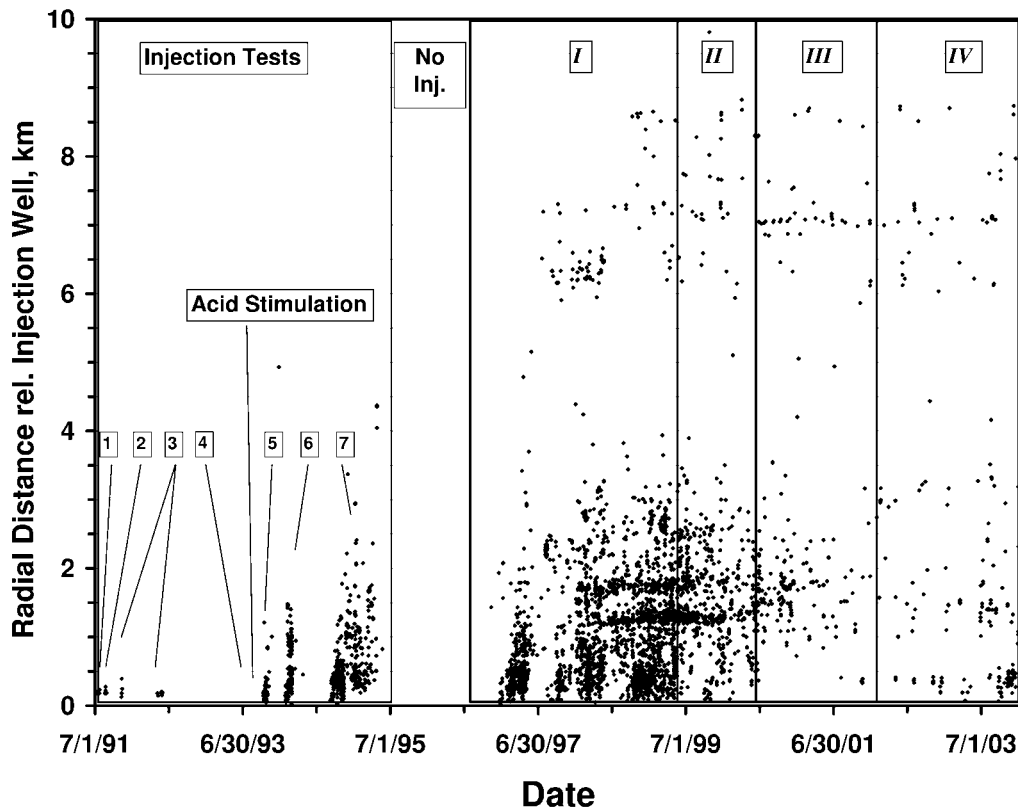
Figure 10. Horizontal distance of induced seismicity from wellbore versus time and injection phase. Initial growth of the two seismogenic zones and their subsequent stasii are shown.

is very active. If the injectate is simply liberating tectonic stress (e.g., reducing normal stress), we expect the seismicity in the zone would gradually decrease. However, with the continuous and high-responsivity of the seismicity, this region may be witnessing a local stress change created by dilation from the invading injectate. As an additional note, the $b$-value for this swarm region is 0.89, which is consistent with the average $b$-value for the Paradox data, as discussed in the next section.

## Earthquake Recurrence

We calculated earthquake recurrence statistics for the period of continuous injection (May 1996–December 2003), and for each of the phases of the continuous injection period. The input data for these calculations are shown in Table 3. The recurrence curves and extrapolation to small magnitude events are shown in Figure 12. The calculations were done using the maximum likelihood method (Weichert, 1980) within estimated confidence bounds (Bollinger *et al.*, 1989); for these calculations we assumed, based on regional tectonics (Ake *et al.*, 2002), a maximum magnitude of **M** 5.5. (Note: These calculations are not particularly sensitive to the maximum magnitude.) Comparing the data in Table 3 and,

assuming a power low relationship between magnitude and number of events is applicable over the range of magnitudes considered here, Figure 12 shows that the data are incomplete for magnitudes less than approximately **M** 0.5.

The extrapolations to smaller magnitudes in Figure 12 suggests that tens of thousands to hundreds of thousands of earthquakes are likely occurring in the magnitude **M** −2 to **M** −3 range. We speculate that this observation has implications for long-term injectate storage, since shear slip across a surface results in imperfect matching of the surfaces (i.e., mismatched asperities and liberated rock particles leave gaps across surfaces) and the creation of new porosity. Hence, slippage across the surfaces of a very large number of small events may pervasively increase the porosity within the rock matrix.

The extrapolation of the Paradox data to small magnitudes represents a lower bound on the number of small events. There may be many more smaller events. The linear extrapolation of this surface-recorded data does not necessarily give an accurate accounting of the number of very small events when compared to in situ monitoring of injection-induced seismicity at the depth of injection. This difference may be due to numerous tensile or fracture opening events that have no analogue in the surface-recorded data (J. Rutledge, personal comm., 2002).
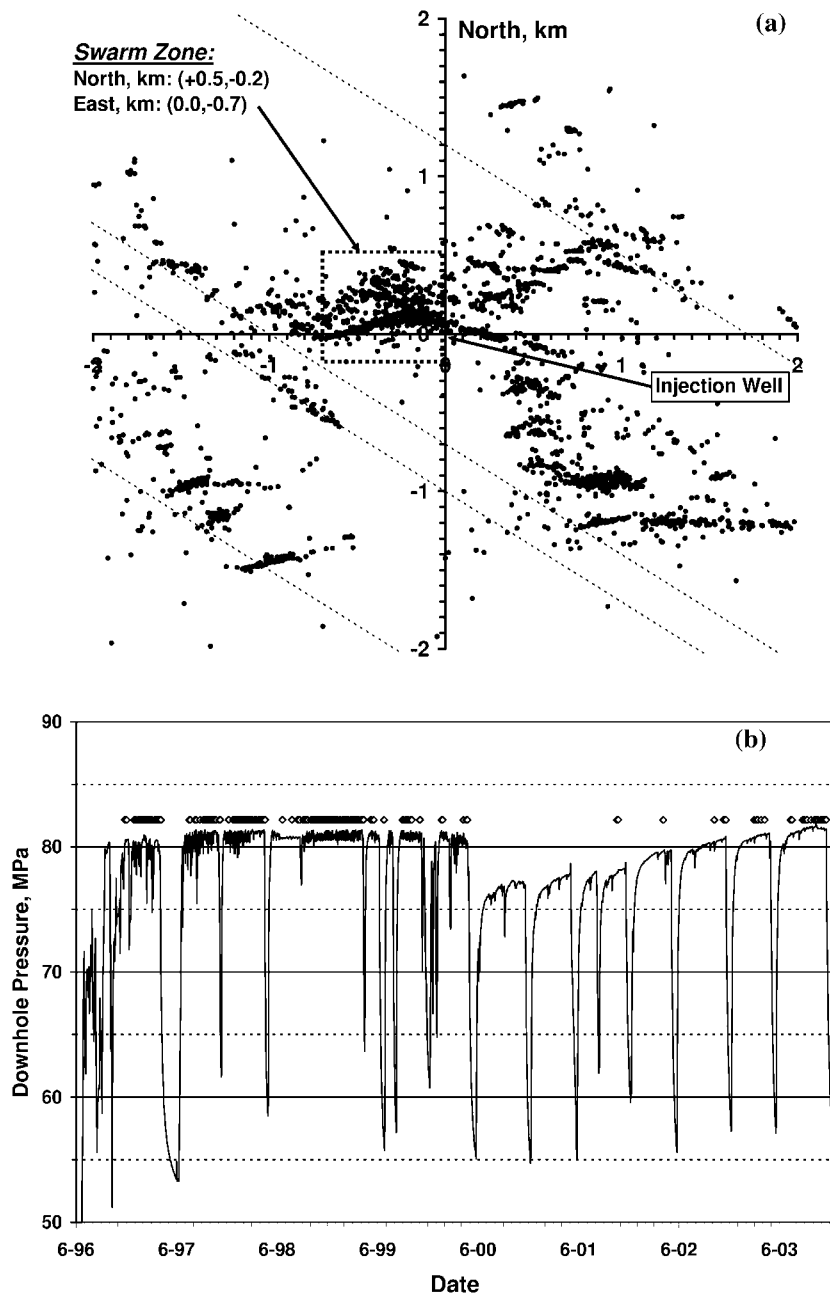
Figure 11. (a) Epicentral map showing swarm (boxed) region, and (b) downhole pressure and occurrence of events in swarm region (diamonds) versus time. Axes centered on injection wellhead.

## Seismic Moment and Injected Volume

The average slope of the recurrence curve, the *b*-value, is 0.82. This value is generally consistent between injection *Phases I* through *III* and with other observations of earthquake occurrence in the Colorado Plateau (Wong *et al.*, 1986; Wong and Humphrey, 1989; LaForge, 1996). The similarity between these PVU *b*-values and other studies in the Colorado Plateau support our conclusion that during *Phases I* through *III*, the large (i.e., surface-recorded), induced events at PVU are from the release of existing tectonic shear stress. However, the *b*-value for *Phase IV* (0.61) is anomalously low. One explanation for this anomaly is that the stress released by these events is not purely tectonic; there may be local stress changes from the massive fluid volume that has been injected.

McGarr (1976) suggested that, for induced seismicity as witnessed at Paradox, the ratio of the sum of the cumulative seismic moment to the cumulative volume is a constant equal to a factor, $K$, close to unity times the shear modulus. McGarr assumes unity for $K$. For limestone, an average value for the shear modulus is $\sim 2 \times 10^{10}$ N/m$^2$ (Clark, 1966). Figure 13 shows the moment-volume ratio for Paradox as a function of time. Also shown are the downhole pressure (pressure at $\sim 4.3$ km depth) and the four pumping phases since 1996. The moment-volume ratio in Figure 13 includes the pump test data, which is the vertical offset from the origin.

Table 3
Number of Events by Magnitude Range and Pumping Phase Used in Calculating Earthquake
Recurrence Curves (Figure 12)

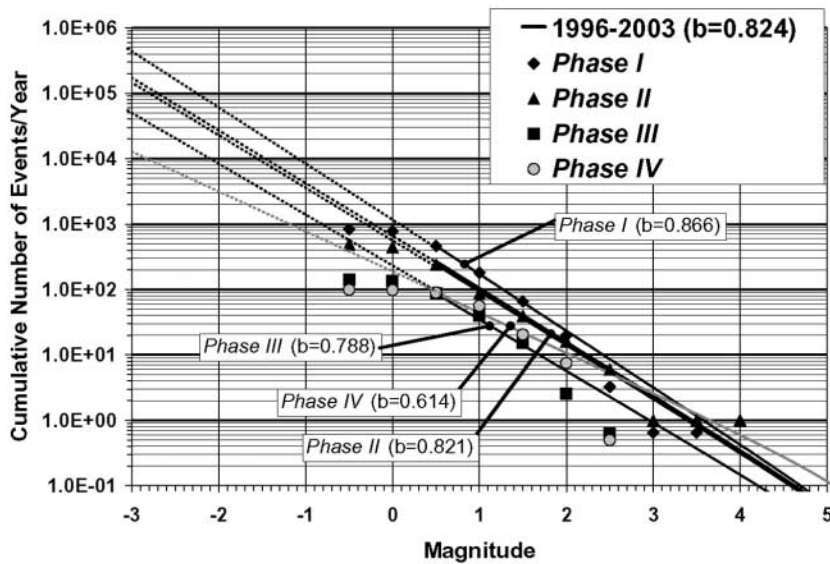| Magnitude Ranges | All (7/96–12/03) no. events | Phase I (7/96–7/99) no. events | Phase II (7/99–7/00) no. events | Phase III (7/00–1/02) no. events | Phase III (1/02–12/03) no. events |
|---|---|---|---|---|---|
| 0.5–0.9 | 1170 | 877 | 152 | 74 | 67 |
| 1.0–1.4 | 513 | 355 | 48 | 39 | 71 |
| 1.5–1.9 | 210 | 141 | 23 | 20 | 26 |
| 2.0–2.4 | 78 | 51 | 11 | 3 | 14 |
| 2.5–2.9 | 16 | 8 | 6 | 1 | 1 |
| 3.0–3.4 | 0 | 0 | 0 | 0 | 0 |
| 3.5–3.9 | 2 | 2 | 0 | 0 | 0 |
| 4.0–4.4 | 1 | 0 | 1 | 0 | 0 |
| b-value | 0.82 | 0.87 | 0.82 | 0.79 | 0.61 |



Figure 12.    Recurrence curves for continuous injection, 1996–2003, showing annualized recurrence for all data and annualized recurrence by injection phase. Dashed lines, extrapolations of data to small magnitude events, 3 + orders of magnitude below detection threshold of surface-based PVSN. Symbols show observed data binned by 0.5 magnitude units.
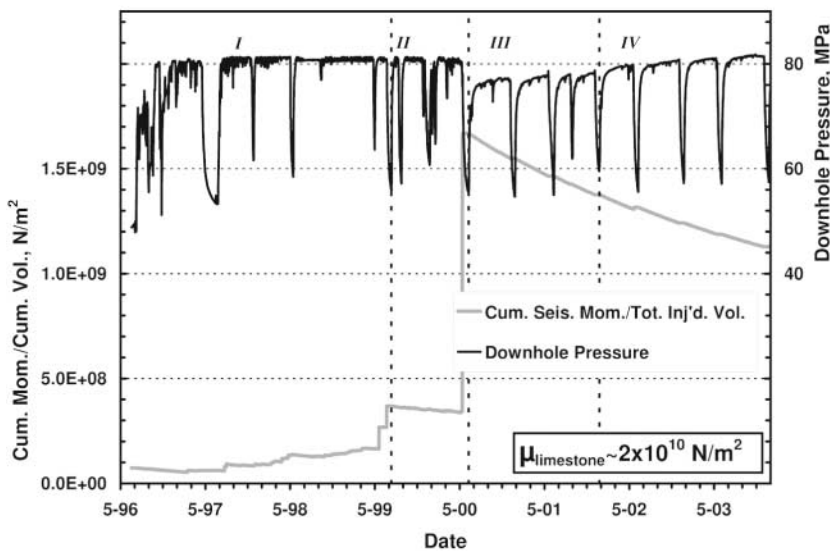


Figure 13.    Ratio of cumulative seismic moment to cumulative injected volume (thick gray line) and downhole pressure (thin black line) versus time. Also shown are the four pumping phases.

In Figure 13, the obvious and large vertical increase in the moment-volume ratio in mid-2000 corresponds to the **M** 4.3 event, and the two small, but still noteworthy "jumps" in the ratio in mid-1999 correspond to the **M** 3.6 and **M** 3.5 events. Figure 13 shows that the moment-volume ratio has not been constant or monotonic, but has increased and decreased between ~$10^8$ and a maximum of ~$1.6 \times 10^9$, immediately following the **M** 4.3 event. Note that with the reduction in injection rate at the inception of *Phase III*, the ratio has been decreasing. In his Discussion section McGarr (1976) states, "It is worth emphasizing that for situations involving fluid injection or withdrawal, [the ratio] is not applicable unless the permeability of the rock is sufficiently low that there is no appreciable fluid flow without fracture." The injection zone at Paradox is highly fractured. We interpret the disparity in the moment-volume ratio as an indication of appreciable fluid flow without fracturing.

## Focal Mechanisms

To evaluate our assumptions regarding the current stress field at the Paradox Valley site and what impact that may have on the injection process, we constructed as many focal mechanisms as possible. The focal mechanism analysis began with 3880 induced events. After application of criteria based on number of observations and solution stability, we obtained 1345 well-constrained focal mechanisms. The Appendix details the method we used to calculate the focal mechanisms.

We defined strike-slip events as those mechanisms where both the *P*- and *T*-axes must plunge less than 25°. Using this criterion, we found 1196 of the 1345 (89%) of the well-constrained events were strike-slip (Fig. 14). We defined oblique focal mechanisms as those mechanisms where the plunge of the *P* (or *T*) axis was greater than or equal to 30°, and the plunge of the corresponding *T* (or *P*) axis was less than 25°. There were 55 normal-oblique events, and 43 reverse-oblique events.

The strike-slip results group into two distinct fault-plane azimuths; a primary set at 266° (86% of the observations), and a secondary set at 311°. For simplicity, we assumed a homogeneous and isotropic medium to interpret the focal mechanisms in terms of stress; a more formal analysis would involve inverting for strain rate (Twiss and Unruh, 1998). We also assumed that the mean *P*- and *T*-axes obtained from samples of the 1345 earthquakes approximately corresponds to the principle stress directions. Assuming reasonable internal friction angles for the Leadville Limestone ($\mu = 0.6$–0.75) suggests a *P*-axis azimuth of 293–296°. This estimate is 27–30° from the primary nodal set azimuth, and within ~15° of the regional *P*-axis azimuth for western Colorado over the past five Ma estimated by Bird (2002).

Hickman and Summers (personal comm., 2003) analyzed televiewer and dipmeter logs, obtained during initial development of the PVU injection well, to estimate borehole breakouts. They estimated the maximum horizontal stress orientation to be 276° ± 5° at Leadville Formation depth based on two successive televiewer runs. They note these results are consistent but may not be accurate. A comparison between borehole televiewer and dipmeter logs showed a maximum difference of 30° between the maximum horizontal stress azimuth estimated from the two sets of logs.

Our estimate of 293–296° for *P*-axis azimuth based on focal mechanisms is within the estimated uncertainty of horizontal maximum shear, $S_{Hmax}$, based on the analysis of televiewer and dipmeter logs. Based on all the observations we estimate a *P*-axis of ~290° ± 10°. This orientation is generally consistent with both *P*-axis estimates (focal mechanism and logs) and with large resolved shear on the both the primary (266°) and secondary (311°) fault-failure planes.

In summary, the focal mechanism results suggest dominately strike-slip failure along a consistent and small number of failure orientations. These agree with the linear pattern of seismicity determined in the relative relocations (Fig. 14). The preferred failure orientation is consistent with other regional stress observations (Bird, 2002), oriented core observations, and analysis of borehole breakouts. This orientation is oblique to the dominant Laramide structural grain. Ake *et al.* (2002) developed focal mechanisms for a number of earthquakes located approximately 85 km to the east of the Paradox Valley, along the boundary between the Colorado Plateau and Southern Rocky Mountains provinces (near Ridgway, Colorado). Their results show mostly normal faulting with a strong indication of east-northeast directed extension. Wong (1986) presented results from an **M** 2.9 earthquake located within the eastern Colorado Plateau near Gateway, Colorado (~35 km north northeast of Paradox Valley) that showed normal faulting with north–northeast-directed extension. The direction of the *P*-axes inferred from the PVSN data is generally similar to the west–northwest-directed compression for the Colorado Plateau (Zoback and Zoback, 1980). However, the PVSN stress orientations, the Gateway earthquake results, and the Ridgway results suggest the eastern Colorado Plateau may be transitional to the extensional southern Rocky Mountains to the east.

As a final note, all focal mechanisms, analyzed to date, are consistent with simple-shear failures. Using the surface-recorded data from PVSN, no tensile or Mode I fractures have been recognized.

## Discussion

Nicholson and Wesson (1990) cite three characteristics for earthquakes induced by injection: proximity, stress state, and pre- and active-injection history. All three have been met at PVU. First, there is a spatial correlation between the zone of fluid injection and the locations of the earthquakes. Second, from the Mohr circle analysis, the inferred state of stress and injection pressure indicate that, at Paradox, the threshold for frictional sliding along favorably oriented fractures has been exceeded. Third, a significant discrepancy exists between seismicity observed prior to injection and
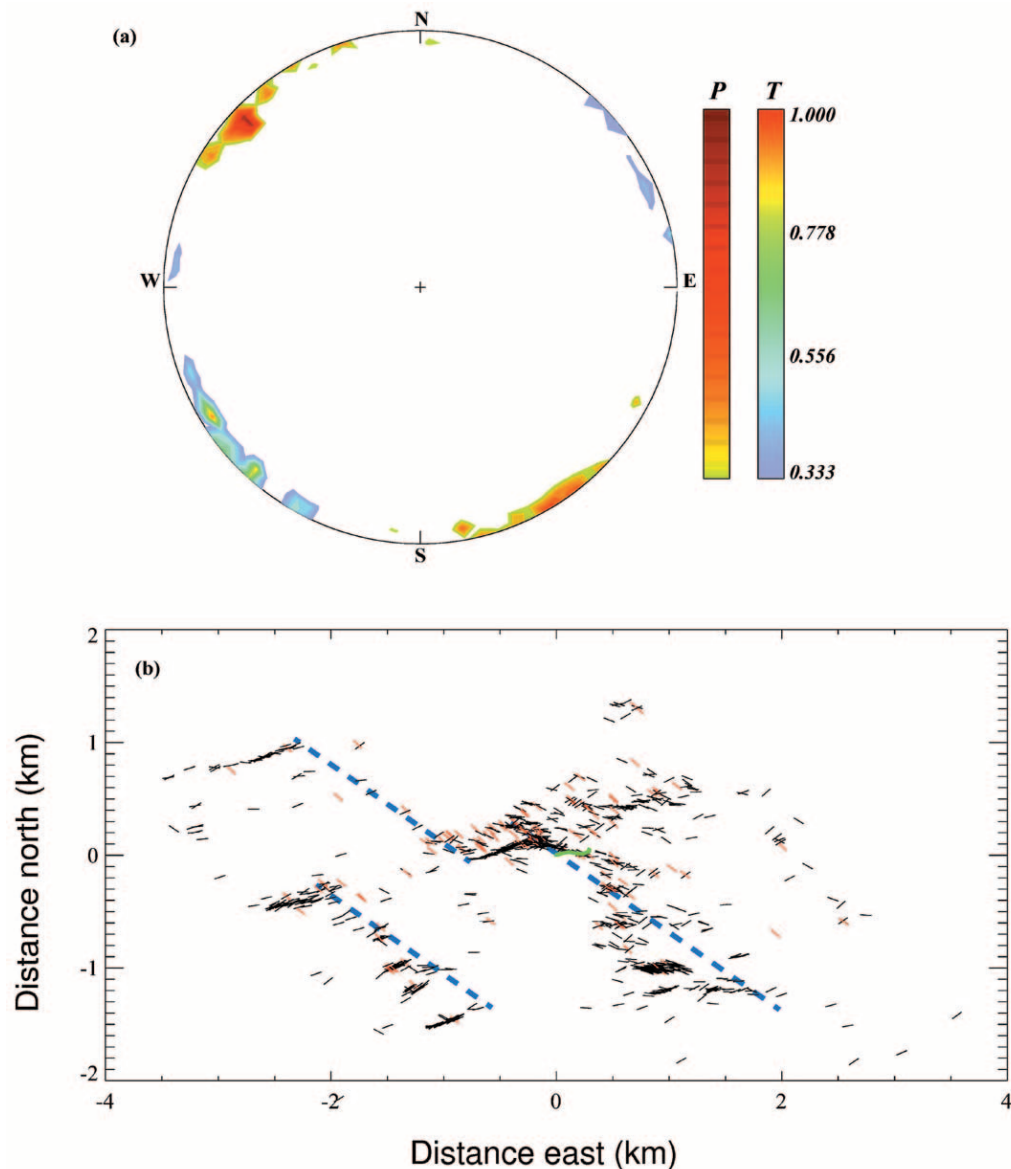
**Figure 14.**   Equal-area densities for *P* and *T* axes from 1196 Earthquakes. (a) Only relative densities of 0.33 or more are plotted. Azimuth-plunge bin size is 4° × 4°. Color bars indicate density relative to the maximum density for *P* axes (red with gray stripes) and *T* axes (blue to red). (b) Dominant (black) and secondary (red) nodal planes in map view. Figure is centered on the injection well wellhead (green line indicates well deviation). Dashed-blue lines are inferred normal-fault locations at the depths of the Leadville Formation.

during injection. Because PVU has a closely-monitored injection history, we note two additional (general) characteristics that demonstrate triggered or induced seismicity at Paradox: a temporal correlation between injection and event hiatuses, and a correlation between event rate and injection intensity.

Recognizing that the seismicity at PVU is induced, we believe that the seismicity at early phases of injection was due to injectate or connate fluids liberating preexisting, in situ tectonic stress across the faults. During the most recent phase of injection, some of the events may be due to chang-

ing the in situ stress by pore and fault inflation from the injectate and migrating connate fluids. Initially, the seismicity was confined to an asymmetric envelope surrounding the injection well. However, after mid-1997, seismicity occurred in two, seismically-distinct event zones: the primary zone (>95% of the events), asymmetrically surrounding the well to a maximum radial distance of ~3 + km; and a secondary zone, displaced ~8 km to the northwest of the injection well along the trend of the previously-identified Wray Mesa fault system. The spatial extent of these zones seems to have stabilized by mid-1999, with the primary zone enclosing a res-

ervoir volume of between 20 and 30 km$^3$. Using an implied seismic envelope based on the earlier hypocenters, the post-1999 seismicity primarily lies in the interior and on the edges of this seismic envelope.

With regard to event size, more than 99.9% of the over 4000 surface-recorded events induced at the Paradox Valley injection since 1991 have magnitudes less than 2.0. The human detection threshold at Paradox seems to be magnitude ~2.6. Approximately 15 events had been felt by the end of 2003. Comparing our data with the at-depth data reported in Phillips *et al.* (2002, figure 1) indicates PVU has probably induced ~2 million events magnitude $-3.0$ and greater. Being a surface array, PVSN's recording sensitivity is ~0.1% of these events.

Throughout its history, the rate of seismicity at Paradox is not uniform; there are extended (i.e., multiday) quiet periods and multihour to multiday active periods and active swarms. Seismic events occur as isolated events and in swarms; with the exception of the swarm zone discussed above, these swarms can last hours to days and lie in a small region (~a few hundred meters of less on a side). Characteristically, these small swarms culminate in one large event and a few foreshocks and aftershocks, or have one large event followed by 5–15 aftershocks.

We found that the earthquakes have been and continue to be confined to a relatively narrow depth range, with many of the hypocenters following the gentle dip (~10°) of the Leadville Formation (Fig. 9) to the northeast. The deepest events occur near the well below the Leadville within the crystalline Precambrian rocks. As shown in Figures 11 and 14, the induced seismicity at Paradox illuminates an extensive system of linear features. These features make up a complex network of faults, fractures, and joints of the Wray Mesa system. Since throughout its history PVU has injected at pressures in excess of the hydraulic fracture pressure, it is interesting to note that the seismically-illuminated fracture and fault system does not conform to the traditional hydraulic fracture model of two vertical symmetric fractures emanating from the opposite sides of the injection well. Using a realistic assumption for fracture aperture (0.5–3 mm) and a height of 500 m (based on the thickness of the perforated interval plus 100 m above and below), the seismically-illuminated faults and fractures can accommodate only a few percent of the injectate volume. The continued storage of injectate is facilitated by the injection pressure continuously opening numerous small fractures (as shown by extrapolation of Fig. 10 to small magnitudes), which provide storage volume and access to pore spaces not accessible from the illuminated fracture and fault system.

The direction of minimum stress (*T*-axis) is consistently northeast and subhorizontal for all events. Fractures observed in oriented core samples recovered during drilling agree with the strike of some of the observed focal planes (Harr, 1988). The lineaments identified in the groupings of relocated events (i.e., the secondary faults and fractures of the Wray Mesa system) have strikes consistent with the fault

planes suggested by the focal mechanisms (Fig. 14). The earthquakes recorded to date are consistent with slip on pre-existing faults or planes of weakness (simple double-couple focal mechanism solutions).

The lack of microearthquake fault planes with orientations parallel to the major, throughgoing faults of the Wray Mesa system suggests these N55°W striking planes may be conduits for fluid transport, but do not have sufficient shear stress to produce earthquakes. We believe they are favorably oriented for dilation (normal to the northeast-directed minimum principal stress) within the inferred stress field.

The production of seismicity at PVU appears to be strongly related to injection rate. Perhaps not surprisingly, we have observed earthquake production for the region within ~2 km of the injection well to be more sensitive to changes in injection rate and shutdown periods than more distant regions (Fig. 11). By evaluating the relationship between earthquake production and injection parameters (injection rate, duration of pumping and injectate chemistry), we have been able to modify operations at PVU to minimize the likelihood of larger, damaging earthquakes.

## Acknowledgments

## References

Ake, J., D. R. H. O'Connell, U. Vetter, and P. S. Chang (1994). Induced microseismicity associated with deep-well disposal of brine at Paradox Valley, Colorado, *EOS Transac. Amer. Geoph. U.* **75,** 473.

Ake, J., D. Ostenaa, K. Mahrer, C. Sneddon, and L. Block (2002). Seismotectonic evaluation and probabilistic seismic hazard evaluation for Ridgway Dam, Dallas Creek Project, Colorado: Seismotectonic Report No. 2001–04, U. S. Bureau of Reclamation, Denver, Colorado, 132 pp.

Baisch, B., M. Bahnhoff, L. Ceranna, Y. Tu, and H.-P. Harjes (2002). Probing the crust to 9-km depth: fluid-injection experiments and induced seismicity at the KTB superdeep drilling hole, Germany, *Bull. Seism. Soc. Am.* **92,** 2369–2380.

Bird, P. (2002). Stress direction history of the western United States and Mexico since 85 Ma, *Tectonics* **21,** doi 10.1029/2001TC001319.

Block, L., J. Ake, and K. Mahrer (2001). The association between seismicity induced by deep-well injection, injectate migration, and tectonic stresses at Paradox Valley, Colorado, *Seism. Res. Lett.* **72,** 286.

Bollinger, G. A., F. C. Davison, M. S. Sibol, and J. B. Birch (1989). Magnitude recurrence relations for the southeastern United States and its subdivisions, *J. Geophys. Res.* **94,** 2857–2873.

Bremkamp, W., and C. L. Harr (1988). Area of least resistance to fluid movement and pressure rise, Paradox Valley Unit, Salt Brine Injection Project, Bedrock, Colorado, a report prepared for the U.S. Bureau of Reclamation, Denver, Colorado, 39 pp.

Clark, S. P., Jr. (Editor) (1966). *Handbook of Physical Constants Revised Edition, Memoir 97,* Geological Society of America, 583 pp.

Cosgrove, J. W. (1995). The expression of hydraulic fracturing in rocks and sediments, in *Fractography: Fracture Topography as a Tool in Fracture Mechanics and Stress Analysis*, M. S. Ameen, (Editor), Geo. Soc. London, Spec. Pub. No. 92, 187–196.

Economides, M. J., and K. G. Nolte (Editors) (1987). *Reservoir Stimulation*, Schlumberger Educational Services.

EnviroCorp (1995). Report of evaluation of injection testing for paradox Valley Injection Test Well No. 1, EnviroCorp Project No. 10Y673, a report to the U.S. Bureau of Reclamation, Denver, Colorado, 26 pp. + figures.

Evans, D. M. (1968). The Denver area earthquakes and the Rocky Mountain arsenal disposal well, *Rocky Mountain Geologist* **3,** no. 1, 101–112.

Goodman, R. E. (1980). *Introduction to Rock Mechanics*, John Wiley and Sons, 478 pp.

Harr, C. L. (1988). Final geological well report, section III—fracture log, a report to the U.S. Bureau of Reclamation, Denver, Colorado.

Healy, J. H., W. W. Rubey, D. T. Griggs, and C. B. Raleigh (1968). The Denver earthquakes, *Science* **161,** 1301–1310.

Hendron, A. J., Jr. (1968). Mechanical properties of rocks, in *Rock Mechanics in Engineering Practice*, K. G. Stagg and O. C. Zienkiewicz (Editors), John Wiley and Sons, 442 pp.

Hseih, P. A., and J. S. Bredehoeft (1981). A reservoir analysis of the Denver earthquakes—a case study of induced seismicity, *J. Geophy. Res.* **86,** 903–920.

Karakha, Y. K., G. Ambats, J. T. Thordsen, and R. A. Davis (1997). Deep well injection of brine from Paradox Valley, Colorado: potential major precipitation problems remediated by nanofiltration, *Water Resources Res.* **33,** 1013–1020.

Kisslinger, C. (1980). Evaluation of S to P amplitude ratios for determining focal mechanisms from regional network observations, *Bull. Seism. Soc. Am.* **70,** 999–1014.

Kisslinger, C., J. R. Bowman, and K. Koch (1981). Procedures for computing focal mechanisms from local (SV/P) data, *Bull. Seism. Soc. Am.* **71,** 1719–1729.

LaForge, R. L. (1996). Seismic hazard assessment for Navajo Dam, Navajo Indian Irrigation Project, New Mexico: Seismotectonic Report No. 96-11, U. S. Bureau of Reclamation, Seismotectonics and Geophysics Group, Technical Service Center, Denver, Colorado, 34 pp.

Mahrer, K. D., (1999). A review and perspective on far-field hydraulic fracture geometry studies, *J. Pet. Sci. and Eng.* **24,** 12–28.

McGarr, A. (1976). Seismic moments and volume changes, *J. Geophy. Res.* **81,** 1487–1494.

Nicholson, C., and R. L. Wesson (1990). Earthquake hazard associated with deep well injection, a report to the U.S. Environmental Protection Agency, *U.S. Geol. Surv. Bull. 1951*, 74 pp.

Phillips, W. S., J. T. Rutledge, L. S. House, and M. C. Fehler (2002). Induced microearthquake pattern in hydrocarbon and geothermal reservoirs: six case studies, *Pure Appl. Geophys.* **159,** N1–3, 345–369.

Press, W. H., S. A. Teukolsky, W. T. Vetterling, and B. P. Flannery (1992). *Numerical Recipes in FORTRAN: The Art of Scientific Computing*, Cambridge Univ. Press, New York, 963 pp.

Raleigh, C. B., J. H. Healy, and J. D. Bredehoeft, (1972). Faulting and crustal stress at Rangely, Colorado, in *Flow and Fracture of Rocks*, H. C. Heard, *et al.* (Editors), American Geophysical Union Monograph 16, 275–284.

Twiss, R. J., and J. R. Unruh (1998). Analysis of fault-slip inversions: do they constrain stress or strain rate? *J. Geophy. Res.* **103,** 12,205–12,222.

Weichert, D. H. (1980). Estimation of the earthquake recurrence parameters for unequal observation periods for different magnitudes, *Bull. Seism. Soc. Am.* **70,** 1337–1346.

Wong, I. G. (1986). Tectonic stresses and their implications to seismicity in Colorado, in *Contributions to Colorado Seismicity and Tectonics— A 1986 Update*, W. P. Rogers and R. W. Kirkham (Editors), Colorado Geological Survey Special Publication No. 28, 17–27.

Wong, I. G., and R. B. Simon (1981). Low-level historical and contemporary seismicity in the Paradox Basin, Utah and its tectonic implications, *Rocky Mountain Association of Geologists Field Conference Guidebook*, 169–185.

Wong, I. G., and J. R. Humphrey (1989). Contemporary seismicity, faulting and the state of stress in the Colorado Plateau, *Geo. Soc. Am. Bull.* **101,** 14–18.

Wong, I. G., S. S. Olig, and J. D. J. Bott (1996). Earthquake potential and seismic hazards in the Paradox Basin, southeastern Utah, *Geology and Resources of the Paradox Basin: Utah Geological Association Guidebook No. 25*, 241–250.

Zoback, M. D., and M. L. Zoback (1980). State of stress in the conterminous United States, *J. Geophy. Res.* **85,** 6113–6156.

Zoback, M. D., and J. H. Healy (1984). Friction, faulting, and in situ stress, *Ann. Geophys.* **2,** 689–698.

## Appendix—Focal Mechanism Method

Focal mechanisms were calculated using *P*-wave first motions and $S_V/P$ amplitude ratios on vertical component seismograms (Kisslinger, 1980; Kisslinger *et al.*, 1981). A simulated annealing downhill simplex algorithm (Press *et al.*, 1992) was used to calculate double-couple focal mechanisms. First motions were weighted 10 times more than $S_V/P$ ratio misfits, and an L1 norm is used to calculate total misfits. The 20% of the $S_V/P$ amplitude ratios with the worst misfit were ignored because $S_V/P$ can become unrealistically large near nodal positions. The velocity seismograms were high-pass filtered with a one pole Butterworth filter at 1 Hz and double integrated to estimate long-period displacement levels. One-second *P*-wave windows and 5-second *S*-wave windows were used to calculate long-period displacement amplitudes. This method of calculating displacement integral amplitudes was compared to spectral fitting procedures to displacement spectra and found to be more stable than spectral approaches. A total of 28 temperature levels were used in the simulated annealing inversions, with a maximum of 90 function evaluations at each temperature. The starting temperature was set to a value corresponding to 60 misfitting first motions and decreased using the temperature schedule, $T = T_0(1 - k/K)^a$ where $T_0$ is the initial temperature, $K$ is the total number of function evaluations, $k$ is the cumulative number of function evaluations so far, and $a$ was set to two. At high temperatures, the process occasionally accepted models associated with increases in functional misfit to inhibit convergence to a local minima. As $T$ tended toward zero, the inversion reduced to a simple downhill simplex algorithm (Press *et al.*, 1992). This approach effectively eliminates the local minima convergence problems Kisslinger *et al.* (1981) experienced with an iterative least-squares inversion approach.

The analysis began with a catalog of 3880 induced

events. The azimuths and takeoff angles from the 3D $P$- and $S$-wave velocity models were used in the focal mechanism calculations. Several criteria were used to determine the quality of estimated focal mechanisms. The first focal mechanism quality filter required a minimum of seven $P$-wave first motions, a total of 12 $S_V/P$ amplitude ratios and $P$-wave first motions, and a first-motion misfit $\leq 0.5$. First-motion misfit was defined as the sum of quality weight factors of first motions with incompatible polarities. Pick qualities of 0 and 1 correspond to impulsive $P$-wave arrivals and pick qualities of 2 and 3 corresponding to increasingly emergent $P$-wave arrivals. The first-motion misfit criteria rejected focal mechanisms with a single pick quality 0 or 1 first-motion misfits, two pick quality 2 first-motion misfits, three quality 3 first-motion misfits, or any combination of quality 2 and 3 first-motion misfits. The criteria of seven $P$-wave first motions establishes reasonable minimum seismogram signal-to-noise ratios. A total of 2145 events passed the first focal mechanism quality filter.

A second quality factor ranked the independence of the focal mechanism solutions to varying starting solutions. Five solutions were obtained for each event, the solution obtained with the starting simplex, and four solutions obtained by inserting trial solutions (strike-slip, normal, reverse, and oblique reverse) as the new starting solution at the end of the previous solution. The filtering criteria required that the maximum differences in $P$- and $T$-axes orientations between the subset of five focal mechanism solutions described above must be $<20°$. The maximum differences in $P$- and $T$-axes orientations were only calculated for event solutions with total L1 misfits no larger than 150% of the minimum misfit. A total of 1345 well-constrained focal mechanisms were obtained after application of the second quality filter.

U.S. Bureau of Reclamation
P.O. Box 25007
Seismotectonics and Geophysics Group, D-8330
Denver Federal Center
Denver, Colorado 80225
  (J.A., K.M., D.O., L.B.)